«WEST» LIKE DIVERTOR GEOMETRY EXPERIMENTS IN ASDEX UPGRADE

O. Meyer[1], E. Belonohy[3], J. Bucalossi[1], R. Dux[3], N. Fedorczack[1], R. Guirlet[1], A. Herrmann[3], A. Kallenbach[3], Y. Marandet[2], S. Potzel[3], M. Sertoli[3] and the ASDEX Upgrade team

[1] *CEA, IRFM, F-13108 Saint-Paul-Lez-Durance, France*

[2] *Aix-Marseille University, CNRS, PIIM, UMR 7345, F-13397 Cedex 20, Marseille, France*

[3] *Max-Planck-Institut für Plasmaphysik, EURATOM-Association, D-85748 Garching, Germany.*

Introduction: The WEST (Tungsten-W Environment in Steady state Tokamak) project aims at equipping the existing Tore Supra device with a Tungsten divertor in order to test actively cooled Tungsten plasma facing components (PFC) in view of preparing ITER operation [Bucalossi11]. The future WEST divertor presents a compact geometry with an X-point close to the W target plate. Tungsten induces strong central radiative losses if transported into the plasma core [Neu13] therefore one question linked to the divertor geometry is its W screening capability. Preliminary experiments were performed at ASDEX Upgrade (AUG) during the 2012 campaign in order to confirm that the WEST shallow divertor geometry does not induce strong operational limitations in a full W device. The first part of the paper describes the settings of the experiments performed; the second discusses the major results obtained.

Plasma configuration and instrumental setup: Two magnetic configurations, shown in figure 1, were tested to match the WEST shallow divertor configuration. The first one uses the lower divertor (LD) roof baffle as a target plate in lower single null configuration (LSN) while the second one uses the upper divertor (UD) in upper single null configuration (USN). Two X-point to target distances: ~2 cm and 7 cm (namely near and far configurations) corresponding to the reference WEST scenarios under study were tested in both cases. For USN experiment, visible and VUV spectroscopic lines of sight shown in figure 1 were available to study respectively W influxes (Γ_W) and W concentration (C_W) in addition to standard background plasma measurements. Figure 2 shows the main plasma parameters for both experiments. The plasma was

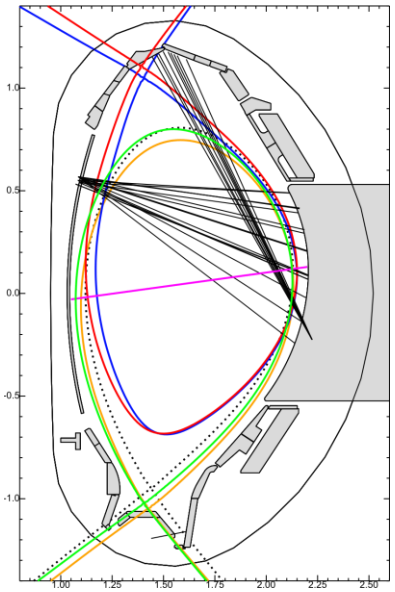

Figure 1: Experimental setup: Separatrix is shown for pulses → 28650;→ 28651;→ 27706; → 27702;-≫AUG; →Visible LOS and →VUV LOS are also shown

heated mainly by neutral beam injection (NBI) with additional electron central heating (ECRH) as usually used in ASDEX to avoid central W accumulation [Neu13]. 2 MW of Ion Cyclotronic Resonance Heating (ICRH), using successively W and Boron (B) coated antennas, were also applied in the USN experiment during the last phases of the discharge. The first 3 seconds (phase 1) of each pulse were used to form a standard AUG LSN geometry and the rest of the pulse was dedicated to the WEST geometry. The level of injected power was higher in the USN pulses (7 MW NBI against 5 MW in LSN). The power injected in the LSN experiment was limited by the appearance of hot spots on misaligned tile leading edges inducing strong W influxes when the NBI power was increased. Larger electronic density was obtained for the LSN experiment (central electronic density of 9 x 10^{19} m^{-3} versus 6 x 10^{19} m^{-3} in USN) as no gas was puffed in the USN configuration to keep a stable density (absence of pumping in the UD). The radiated power increase during the phase 2 of the LSN configuration is attributed to light impurities released from the incompletely conditioned roof baffle tiles. A first result is that the X-point height seems not to affect the global plasma parameters during the NBI + ECRH phase while an effect is observed during the NBI + ICRH phase.

Main observations and results: The main result is that ELMy H-mode was achieved and sustained during the WEST phase of both experiments but differences are observed between the AUG and the WEST configurations as shown in table 1. In the LSN geometry, a NBI power ramp from 0 to 5 MW allowed us to determine that the L-to-H transition threshold is about 2 MW, slightly above the 1.5 MW expected in a standard AUG configuration. Scaled to the WEST magnetic field (3.6 T instead of 2.4 T in this experiment), we estimate the threshold in WEST to be around 3.4 MW that is well within the injected power capability of WEST. Note that the global confinement (H_{98}) in WEST geometry is similar (lower in LSN configuration cases due to high gas puffing values) to the one in standard AUG LSN configuration (phase 1). Regarding W behaviour, the figures 3 and 4 show respectively the W sources on the main W

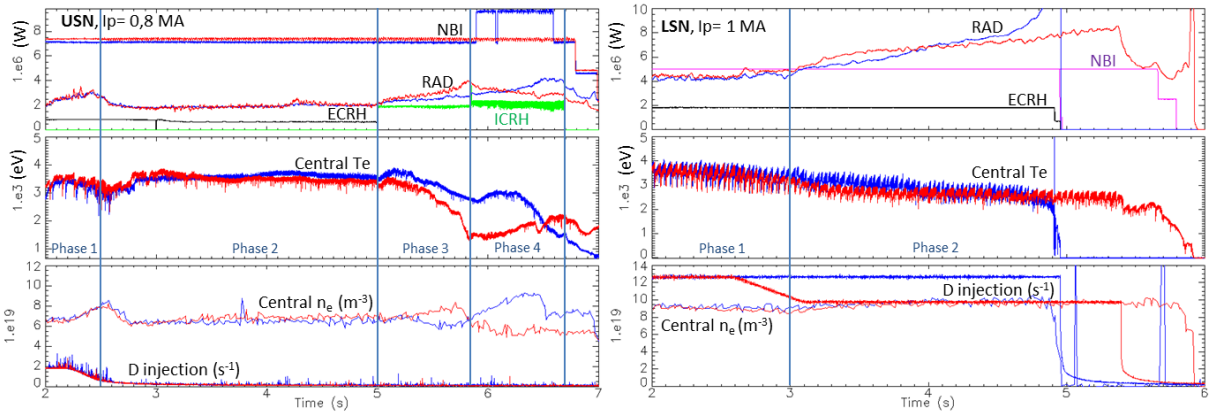

Figure 2: main plasma parameters for shots in LSN: 27702 (far) and 27706 (near) and in USN: 28650 (far) and 28651 (near); → Near configuration, → Far configuration; pulse phases are also indicated

Table 1: Characteristics of H-mode during WEST like geometry phases

Configuration		H_{98}	N_{ELMS} (Hz)	Prad (MW)	P_{IN} (MW)	L-H threshold (MW)	Phase
LSN AUG	NBI + ECRH	0.8	60	4	7	1.5	1
LSN 2 cm	NBI + ECRH	0.8	200	5 to 7	7	2	2
LSN 7 cm	NBI + ECRH	0.8	200	5 to 7	7		2
USN 2 cm	NBI + ECRH	1	100	2	8.1		2
	NBI + ICRH (W)	1	150	4	9		3
	NBI + ICRH (B)	0.7	250	2.5	9		4
USN 7 cm	NBI + ECRH	1	200	2	8.1		2
	NBI + ICRH (W)	1	225	3	9		3
	NBI + ICRH (B)	1	250	4	12		4

internal components and the W content evolutions during the pulse for the USN configuration. The time integrated flux along the pulse (W neutrals / m²) is presented to compare signals with low acquisition sampling period regarding ELM frequency as it is the case for the UD system (set up especially for the experiment and performing 20 ms sampling period compared to an ELM period down to 5 ms), averaged W influxes are estimated by using the derivative of the curves. The first point to mention is the unexpectedly low W influxes measured on the UD since for the far configuration case a $\Gamma_W \sim 1.6 \times 10^{18}$ neutrals / m^2.s is estimated instead of $\sim 10^{19}$ neutrals / m^2.s for the LD during the phase 2. That point could be due to insufficient conditioning of the UD or a misalignment of the coated tiles inducing a major flux deposit on the Carbon edges (significant C III influxes are measured). This experiment therefore cannot help to predict the W source from the divertor in WEST. The second point to mention is the strong difference of the LD induced W influxes between the near and far configuration (Γ_W of 1.5×10^{20} versus 10^{19} neutrals / m^2.s estimated during the phase 2). The difference is a probable consequence of the size of the ELMs. Indeed, the ELMs are identified as type I and they present in the phase 2 a frequency of 100 Hz for the near configuration to be compared with 200 Hz for the far configuration. During the phase 4, an ELM frequency of 250 Hz is measured along with similar Γ_W in both cases. Regarding the W plasma content, C_W at 1 keV is stable in both cases but is a factor of 2.5 larger in the near configuration that is probably due to the additional LD W influxes. C_W at 3 keV increases quickly from 2×10^{-5} to 10^{-4} in both cases, signature of W accumulation [Neu13] even if central T_e and n_e are not affected at that time of the pulse. In phase 3, additional W influxes from the W coated antenna limiters appear and the estimated Γ_W are 1.9×10^{19} and 1.6×10^{19} neutrals / m^2.s for the near and far configuration to be compared to $\sim 7 \times 10^{18}$

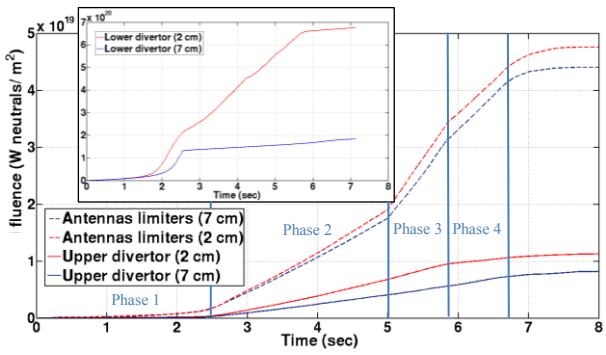

Figure 3: W time integrated fluxes for W antenna limiters, upper and lower divertors

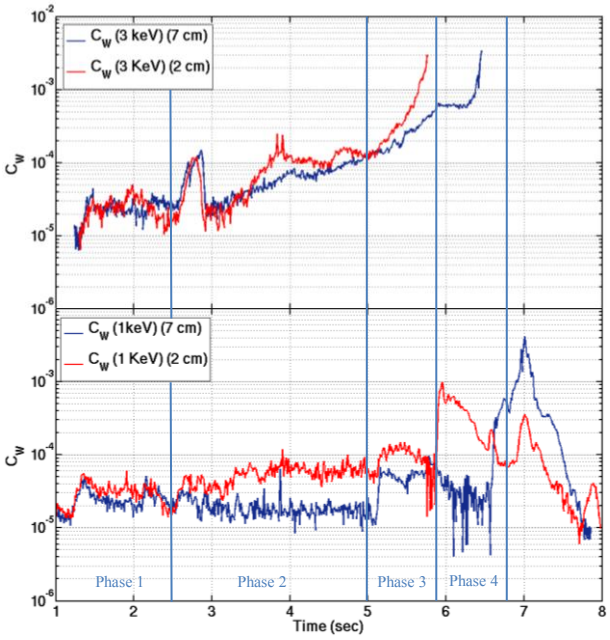

Figure 4: C_W at r_{plasma} (T_e=1 KeV) and r_{plasma} (T_e=3 KeV) for near (28651) and far (28650) configurations

neutrals / m^2.s for both cases in phase 2. C_W at 1 keV undergoes a sharp increase in both cases (about a factor of 2) but the C_W at 3 keV reveals a W accumulation higher in the near configuration than in the far one. The W peaking strongly affects the background plasma in both cases since drops of the central T_e from 3.6 to 2.7 keV and from 3.2 to 1.5 keV are observed in the far and near configurations respectively. The phenomenon of W accumulation with W coated antennas has already been observed during standard AUG pulses and is linked to the increase of the W influxes that compensate the beneficial effect of central heating [Neu13]. The lower ELM frequency of the near configuration is possibly the reason of the lower performances observed since it induces additional W influxes and frequent ELMs are beneficial in keeping a low W level in the plasma. During the phase 4 where ICRH with B coated antenna limiters is applied, Γ_W is reduced and C_W at 1 keV decreases by a factor of 10 for the near configuration as long as a central T_e increases showing the beginning of a plasma recovering.

Conclusion: Two X-point geometries, near (2 cm height) and far (7 cm height) in USN and LSN configurations, were addressed during AUG experiments. A sustained ELMy H-mode was achieved for both configurations and we determined L-H threshold of 2 MW (~ 3.2 MW on WEST) for the LSN configuration. Regarding W control, stable plasma performances were maintained during NBI + ECRH phases for both configurations but degradations occurred during the NBI + ICRH (W coated antennas) phases especially for the near X-point configuration. The issues were both W influxes induced by ELMs in the lower divertor along with W coated antennas and W concentration peaking occurring after ECRH stop. The beginning of a plasma recovery was observed when switching to B coated antennas where central heating was applied with lower W influxes. These preliminary experiments on AUG give good confidence in the H-mode feasibility in WEST geometry and identify some points to stress on in view of WEST operation, namely: ICRH induced W influxes reduction, ECRH system optimization to reduce W accumulation and control of ELM induced W sources.

[Bucalossi11] J. Bucalossi et al., Fusion Engineering and Design 86 (2011) 684–688

[Neu13] R. Neu et al., J. Nucl. Mater. (2013)